

# Alcohol Denaturation: Thermodynamic Theory of Peptide Unit Solvation

Seishi Shimizu\* and Kentaro Shimizu

Contribution from the Bioinformation Engineering Laboratory, Department of Biotechnology, The University of Tokyo, 1-1-1 Yayoi, Bunkyo-ku, Tokyo 113-8657, Japan

Received July 20, 1998

**Abstract:** Although destabilization of solvent-exposed amide groups in the coil state has been shown to be the main factor involved in helix induction in alcohol denaturation, no theory has been proposed that describes the alcohol concentration dependence of denaturation. This paper presents a theory that can describe transfer free energies of a peptide backbone unit from water to aqueous alcohol solutions of various compositions. This theory is an indispensable step in the quantitative description of the solvent roles in alcohol denaturation. The theory is based on the definition of the molarity-based transfer free energy and is made up of following two contributions: (1) free site transfer, which is shown basically to be the cavity formation term, and (2) solvent exchange coming from competition of hydrogen bonding of solvents to the peptide. The theoretical transfer free energies successfully reproduce, at a low alcohol concentration range, the experimental values for the case of aqueous methanol and ethanol solvents, where excluded-volume effects are shown to play the dominant role. The theory has further been applied to 2,2,2-trifluoroethanol (TFE), for which experimental values of peptide transfer free energy are not available. The theory goes beyond the Tanford scheme by introducing conditional solvation of the peptide unit by side chains and successfully describes the TFE concentration dependence of the peptide transfer free energy, which reflects the dependence of helix induction curve.

## 1. Introduction

It has long been known that the addition of alcohol destabilizes the native structure of proteins and stabilizes secondary structures<sup>1–3</sup>. The characterization of such denatured states has been extensively investigated because of its critical importance to the description of the protein folding mechanism<sup>4–9</sup>. Understanding the mechanism by which solvents stabilize secondary structures would provide an insight into the fundamental interactions in protein structure stabilization.<sup>23</sup> Recently, the effect of 2,2,2-trifluoroethanol (TFE) has extensively been investigated experimentally<sup>12–20</sup> and theoretically<sup>18,21,22</sup> because

of TFE's great effectiveness<sup>23</sup> in the stabilization of the  $\alpha$ -helix and other secondary structures such as  $\beta$ -hairpins.<sup>24</sup>

The classical formalism of Tanford<sup>2</sup> enables one to calculate the free energy of denaturation. Based on the experimental transfer free energy  $\Delta g_i$  of each constituent group  $i$ , the free energy of denaturation can be calculated by  $\Delta G = \sum_i n_i (\Delta \alpha_i) \Delta g_i$ , where  $\Delta \alpha_i = \alpha_i(\text{h}) - \alpha_i(\text{c})$  is the difference of fractional exposure of the group  $i$  to the solvent  $\alpha_i$  between helix (h) and coil (c) states and  $n_i$  is the number of  $i$ th group species. This formalism assumes the group additivity of the solvation free energy. Experimental values of  $\Delta g_i$ 's determined from solubility measurements have been reported for ethanol,<sup>25–28</sup> methanol,<sup>26</sup> and some polyols<sup>2,27,29</sup> (there have been no corresponding data reported for TFE). Since  $\Delta \alpha_{\text{hydrophobic}} = 0$  for hydrophobic side chains in the helix-coil transition,<sup>2</sup> the stabilization of the helix states comes from the positive  $\Delta g_{\text{peptide}}$  and the reduction of peptide unit exposure upon helix formation  $\Delta \alpha_{\text{peptide}} = -0.35$ .<sup>2,29</sup> What is, then, the molecular mechanism that makes  $\Delta g_{\text{peptide}}$

\* Corresponding author: (e-mail) seishi@bi.a.u-tokyo.ac.jp; (phone) +81-3-3813-8728; (fax) +81-3-3813-8723.

(1) Conio, G.; Patrione, P.; Brighetti, S. *J. Biol. Chem.* **1970**, *245*, 3335.  
 (2) Tanford, C. *Adv. Protein Chem.* **1970**, *25*, 1.  
 (3) Kauzmann, W. *Adv. Protein Chem.* **1954**, *14*, 1.  
 (4) Kim, P. S.; Baldwin, R. L. *Annu. Rev. Biochem.* **1990**, *59*, 631.  
 (5) Dill, K. A.; Shortle, D. *Annu. Rev. Biochem.* **1991**, *60*, 795.  
 (6) Thomas, P. D.; Dill, K. A. *Protein Sci.* **1993**, *2*, 2050.  
 (7) Fersht, A. R. *FEBS Lett.* **1993**, *325*, 5.  
 (8) Buck, M.; Schwalbe, H.; Dobson, C. M. *J. Mol. Biol.* **1996**, *257*, 669.  
 (9) Kamatari, Y. O.; Konno, T.; Kataoka, M.; Akasaka, K. *Protein Sci.* **1998**, *7*, 681.  
 (10) Nelson, J. W.; Kallenbach, N. R. *Proteins* **1986**, *1*, 211.  
 (11) Storrs, R. W.; Truckses, D.; Wemmer, D. E. *Biopolymers* **1992**, *39*, 1695.  
 (12) Jasanoff, A.; Fersht, A. R. *Biochemistry* **1994**, *33*, 2129.  
 (13) Kuprin, S.; Graeslund, A.; Ehrenberg, A.; Koch, M. H. *J. Biochem. Biophys. Res. Commun.* **1995**, *217*, 1151.  
 (14) Luodens, M. K.; Figge, J.; Breeze, K.; Vajda, S. *Biopolymers* **1996**, *39*, 367.  
 (15) Rohl, C. A.; Chakraborty, A.; Baldwin, R. L. *Protein Sci.* **1996**, *5*, 2623.  
 (16) Cammers-Goodwin, A.; Allen, T. J.; Oslick, S. L.; McClure, K. F.; Lee, J. H.; Kemp, D. S. *J. Am. Chem. Soc.* **1996**, *118*, 3082.

(17) Kemp, D. S.; Allen, T. J.; Oslick, S. L.; Boyd, J. G. *J. Am. Chem. Soc.* **1996**, *118*, 4240. Kemp, D. S.; Oslick, S. L.; Allen, T. J. *J. Am. Chem. Soc.* **1996**, *118*, 4249.

(18) Bodkin, M. J.; Goodfellow, J. M. *Biopolymers* **1996**, *39*, 43.  
 (19) Luo, P.; Baldwin, R. L. *Biochemistry* **1997**, *36*, 8413.  
 (20) (a) Hirota, N.; Mizuno, K.; Goto, Y. *Protein Sci.* **1997**, *6*, 416. (b) Hirota, N.; Mizuno, K.; Goto, Y. *J. Mol. Biol.* **1998**, *275*, 365.  
 (21) De Loof, H.; Nilsson, L.; Rigler, R. *J. Am. Chem. Soc.* **1992**, *114*, 4028.  
 (22) Brooks, C. L., III; Nilsson, L. *J. Am. Chem. Soc.* **1993**, *115*, 11034.  
 (23) Rajan, R.; Balaran, P. *Int. J. Protein Pept. Res.* **1996**, *48*, 328.  
 (24) Schoenbrunner, N.; Wey, J.; Engels, J.; Georg, H.; Kiefhaber, T. *J. Mol. Biol.* **1996**, *260*, 432.  
 (25) Nozaki, Y.; Tanford, C. *J. Biol. Chem.* **1971**, *246*, 2211.  
 (26) Gekko, K. *J. Biochem.* **1981**, *90*, 1633.  
 (27) Nozaki, Y.; Tanford, C. *J. Biol. Chem.* **1965**, *240*, 3568.  
 (28) Conio, G.; Curletto, L.; Patrone, E. *J. Biol. Chem.* **1973**, *248*, 5448.  
 (29) Liu, Y.; Bolen, D. W. *Biochemistry* **1995**, *34*, 12884.

positive for an alcohol–water mixture? Tanford's theory does not provide a direct answer to this question. We must develop a theory that can describe  $\Delta g_{\text{peptide}}$  (and predict  $\Delta g_{\text{peptide}}$  for the system, such as TFE, where no experimental value has been obtained) solely from basic physicochemical properties such as mixing properties and hydrogen bond strengths. Such a description would be of great importance because it would give us an understanding of the molecular mechanism of denaturation.

The molecular mechanism of alcohol denaturation has extensively been investigated, especially for TFE, because of its effectiveness in helix induction. Various possibilities have been proposed for the mechanism of alcohol denaturation: (1) dielectric effect, (2) helix stabilization by direct binding of TFE,<sup>12</sup> and (3) coil destabilization by destabilizing exposed amide groups.<sup>1,11,16</sup> In the dielectric effect, the addition of alcohols lowers solvent polarity and thus strengthens intramolecular hydrogen bonding. Several experimental results, however, suggest that this picture is too simple<sup>1,10,20</sup> and may not be the major contributor for the following reasons: first, while the increase of helicity by aliphatic alcohols has similar linear dependence on the dielectric constant, TFE contributes much more to helix induction than do these alcohols.<sup>20</sup> The dielectric effect cannot give a unified explanation that can be applied to various species of alcohols. Second, the effect of a charged group, which is expected to be altered significantly by polarity, was only slightly altered over various concentrations of TFE for ribonuclease S-peptide.<sup>10</sup> Helix stabilization by direct binding of TFE<sup>12</sup> fits the experimental data in which helicity becomes saturated at a relatively low concentration of TFE. However, the molecular picture of this direct binding mechanism remains unclear. Moreover, this picture contradicts NMR evidence reported by Storrs et al.,<sup>11</sup> which does not support direct or indirect stabilizing interactions of TFE with the helical states. The possibility of coil destabilization by exposed amide groups was originally proposed by Conio et al.<sup>1</sup> as the mechanism of helix enhancement in aliphatic alcohols. Storrs et al.<sup>11</sup> suggested from NMR measurement that this also holds in a TFE–water mixture. Furthermore, Cammers-Goodwin et al.<sup>16</sup> suggested, by NMR and CD measurements of short peptides, that the coil destabilization is enhanced by the solvation state of the exposed amides (part of peptide unit) that promotes helix induction. This is consistent with the picture derived from Tanford's theory, that the destabilization of the solvent-exposed amide group is the main contribution to the coil destabilization. Then how can this picture of peptide unit destabilization, in turn, describe the TFE concentration dependence of the helicity? Can it really be described within the framework of the Tanford scheme where group additivity is assumed? The molecular theory of transfer free energy would again provide decisive means of answering these questions.

Transfer free energies have been shown to be made up of cavity formation and attractive interactions.<sup>34–37</sup> The cavity

(30) *International Critical Tables*; McGraw-Hill: New York, 1925; Vol. III.

(31) Rochester, C. H.; Symonds, J. R. *J. Fluorine Chem.* **1974**, *4*, 141.

(32) Butler, J. A. V.; Thomson, D. W.; MacLennan, W. H. *J. Chem. Soc.* **1933**, 674.

(33) Smith, L. S.; Tucker, E. E.; Christian, S. D. *J. Phys. Chem.* **1981**, *85*, 1120.

(34) Barker, J. A.; Henderson, D. *Rev. Mod. Phys.* **1976**, *48*, 587.

(35) Reviews of this topic are: (a) Chan, H. S.; Dill, K. A. *Annu. Rev. Biophys. Biomol. Struct.* **1997**, *26*, 425. (b) Sanchez-Ruiz, J. M. *Eur. Biophys. J.* **1996**, *24*, 261. (c) Ben-Naim, A. *Curr. Opin. Struct. Biol.* **1994**, *4*, 264.

(36) (a) Shimizu, S.; Ikeguchi, M.; Shimizu, K. *Chem. Phys. Lett.* **1998**, *282*, 79. (b) Shimizu, S.; Ikeguchi, M.; Nakamura, S.; Shimizu, K. *Chem. Phys. Lett.* **1998**, *284*, 235. (c) Shimizu, S.; Ikeguchi, M.; Nakamura, S.; Shimizu, K. *J. Chem. Phys.* **1999**, *110*, 2971.

formation free energy in the alcohol–water mixture is determined from the following two contributions. (1) The addition of alcohols would generally increase the mean molecular size of the solvent and would contribute to the decrease in the cavity formation free energy. Although the physical origin of the hydrophobic effect (large positive cavity formation free energy in water) is not yet fully understood, we have confirmed in our recent paper<sup>37</sup> that the free energy of cavity formation at a given density is mainly determined by the hard core of water: the free energy of cavity formation at a given density in water was found to be similar to that in the Lennard-Jones fluid of the same density. This supports the proposal by Lee<sup>38</sup> for the hard-sphere scaled particle theory (SPT) that the small size of the hard core of water is responsible for the hydrophobic free energy, i.e., large positive cavity formation free energy. Therefore, the increment of the mean solvent radius upon the addition of alcohols is expected to lower the free energy of cavity formation. (2) The addition of alcohols would also increase the solvent density and packing fraction.<sup>31</sup> This would increase the cavity formation free energy. This interplay between effects of solvent density and solvent size<sup>36</sup> is expected to take place also in the case of peptide transfer. For attractive interactions, the hydrogen-bonding ability of water and alcohols to peptide CO and NH would cause the free energy of the solvent exchange and has been proposed by Schellman as a model for denaturation in much simpler systems.<sup>39</sup> However, contributions other than solvent exchange, such as cavity formation, have been ignored in his theory and the binding parameters in his theory have merely been fitting parameters. To obtain a complete theory of transfer, we must generalize Schellman's formalism into the new formalism presented in section 2, which is based on a molarity-based concentration scheme<sup>40</sup> that incorporates hydrogen bonding as well as other interactions such as cavity formation. The theory is able to reproduce the experimentally measured  $\Delta g_{\text{peptide}}$  of methanol and ethanol<sup>2</sup> at lower concentrations of alcohols. We also applied it to the aqueous TFE system in section 3 in order to clarify the molecular mechanism of helix induction by TFE.

## 2. Theory

In this section, we present a theory that describes transfer free energy of a peptide from pure water to an aqueous alcohol mixture based solely on the mixing properties of the alcohol–water mixture (activities and density) and hydrogen bond strengths between peptide and solvent components. Everything presented in this section refers to one site for simplicity and is supposed to be summed over sites to obtain the total contributions from the peptide group.

**2.1. General Formalism for Hydrogen Bonds.** Consider the transfer of a site from a fixed position in pure water (phase 0) to a fixed position in an aqueous alcohol mixture (phase m). The transfer free energy is expressed by the theory of Ben-Naim<sup>40</sup> as

$$\Delta G^* = -RT \ln \left[ \frac{[P]_m}{[P]_0} \right] \quad (1)$$

(37) Ikeguchi, M.; Shimizu, S.; Nakamura, S.; Shimizu, K. *J. Phys. Chem. B* **1998**, *102*, 5891.

(38) Lee, B. *Biopolymers* **1985**, *24*, 813. Lee, B. *Biopolymers* **1991**, *31*, 993.

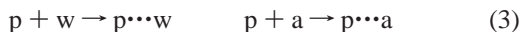
(39) Schellman, J. A. *Biopolymers* **1987**, *26*, 549. Schellman, J. A. *Biophys. Chem.* **1990**, *37*, 121. Schellman, J. A. *Biophys. Chem.* **1993**, *45*, 273. Schellman, J. A. *Biopolymers* **1994**, *34*, 1015. Schellman, J. A.; Gassner, N. C. *Biophys. Chem.* **1996**, *59*, 259.

(40) Ben-Naim, A. *Statistical Thermodynamics for Chemists and Biochemists*; Plenum: New York, 1992.

where  $[[P]]_0$  and  $[[P]]_m$  express the number density of the sites in pure water and aqueous alcohol mixtures, respectively, and can be expressed as the following sum of “solvation states”:  $[p]$  (non-hydrogen-bonded states),  $[p\cdots w]$  (hydrogen bonded by water), and  $[p\cdots a]$  (hydrogen bonded by alcohol), as

$$\begin{aligned} [[P]]_0 &= [p]_0 + [p\cdots w]_0 \\ [[P]]_m &= [p]_m + [p\cdots w]_m + [p\cdots a]_m \end{aligned} \quad (2)$$

These species are formed by the following stoichiometric reaction:



Now we assume an infinite dilution limit of the sites. The activity of the sites becomes identical to mole fraction, and the number density becomes proportional to mole fraction. The equilibrium constant can then be written for the above reaction as,

$$K_w = [p\cdots w]/[p][w] \quad K_a = [p\cdots a]/[p][a] \quad (4)$$

where  $[a]$  and  $[w]$  are the activities of alcohol and water, respectively. The  $K$ s are constants independent of solvent composition.

Combining the eqs 1, 2, and 4, the transfer free energy becomes,

$$\Delta G^* = -RT \ln \frac{[p]_m}{[p]_0} - RT \ln \left( \frac{1 + K_w[w]_m + K_a[a]_m}{1 + K_w} \right) \quad (5)$$

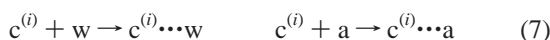
$$\approx -RT \ln \frac{[p]_m}{[p]_0} - RT \ln \left( [w]_m + \frac{K_a}{K_w} [a]_m \right) \quad (6)$$

What is the physical interpretation of eq 5? The first term expresses the transfer of a free site from the pure water phase 0 to the aqueous alcohol solution m. This contribution has been neglected by Schellman<sup>39</sup> since the partition function of a free site was set to 1 in the binding polynomials in the theory of Schellman. Our thermodynamic formalism is able to clarify this contribution. The second term expresses the effect of solvent exchange derived by Schellman<sup>39</sup> (in the second term of eq 6, the final result of Schellman can be obtained by the assumption that the number of free sites is small compared to the number of hydrogen-bonded sites). The binding constants in the Schellman theory are fitting parameters: the parameters are determined from hydrogen-bonding strengths in section 3 of this paper and have a clear physical meaning. To summarize, we have developed a complete theory of transfer free energy based on molarity scale, which contains both solvent exchange and free site transfer.

**2.2. Transfer of a Free Site.** How can we calculate the free site transfer,  $\Delta G^*_{\text{free}}$ , the first term of eq 5?

We first note that  $\Delta G^*_{\text{free}}$  is composed of solute–solvent van der Waals interaction and the free energy of cavity formation. If we assume that the van der Waals interaction can be expressed in terms of a stoichiometric reaction model, the “free site”  $[p]$  is considered to be composed of  $n$  independent binding sites of van der Waals interaction.

The following stoichiometric reactions and the equilibrium constants are assumed for this van der Waals binding:



and

$$K'_w = [c\cdots w]^{(i)}/[c]^{(i)}[w] \quad K'_a = [c\cdots a]^{(i)}/[c]^{(i)}[a] \quad (8)$$

where  $[c\cdots w]^{(i)}$ ,  $[c\cdots a]^{(i)}$ , and  $[c]^{(i)}$ , respectively, express the  $i$ th site bonded by water, by alcohol, or not bonded at all.

$\Delta G^*_{\text{free}}$  is given as,

$$\Delta G^*_{\text{free}} = -RT \ln \frac{[c]_m}{[c]_0} - nRT \ln \left( [w]_m + \frac{K'_a}{K'_w} [a]_m \right) \quad (9)$$

where we have assumed that all the binding sites are equal and  $\prod [c\cdots a]^{(i)} = [c]$ .

The first term of eq 9 expresses the change of cavity formation free energy between the phases 0 and m, whereas the second term expresses the change of van der Waals interaction. Since van der Waals interaction is much weaker than hydrogen bonding, and taking into account the size difference between alcohol and water,  $K'_a/K'_w$  is expected to be small. The leading term in the logarithm of the second term of eq 9,  $[w]$ , decreases very slowly, in comparison to ideal solution, with the increment of alcohol concentration in the lower concentration range of alcohols, as is shown in Figure 1a. It is therefore expected that the second term in eq 9 cannot deviate greatly from zero at the lower concentration range of alcohols and may therefore be ignored. This assumption will later be justified by the fact that theoretical prediction at lower alcohol concentration reproduces the experimental transfer free energies.

Another justification for ignoring the second term of eq 9 comes from the assumption that the solvent structure around a site is almost identical to the structure around a “cavity” of the site, which is justified by the successful applications of perturbation theories to multicomponent fluids.<sup>34</sup>

The excess number of water molecules in the solvation shell of a site<sup>39</sup> is thus expected to be equal to that of a cavity, i.e.,

$$\left( \frac{\partial N_w}{\partial N_s} \right)_{T, \mu_w, \mu_a} = \left( \frac{\partial N_w}{\partial N_s} \right)_{T, \mu_w, \mu_a}^{(\text{cav})} \quad (10)$$

where  $N_w$  and  $N_s$  are the number of water molecules and sites in the whole system and the  $\mu$ 's are the chemical potentials of each component. Note that (cav) denotes cavity.

By Stigler's approximation,<sup>42</sup>  $\left( \frac{\partial N_w}{\partial N_s} \right)_{T, \mu_w, \mu_a} \approx \left( \frac{\partial N_w}{\partial N_s} \right)_{T, P, \mu_w}$ , which is frequently used in preferential solvation measurements,<sup>43</sup> and the thermodynamic relationship  $\left( \frac{\partial N_w}{\partial N_s} \right)_{T, P, \mu_w} = -\left( \frac{\partial \mu_s}{\partial \mu_w} \right)_{T, P, N_s}$ , we can transform eq 10 into the following form:

$$\left( \frac{\partial \mu_s}{\partial \mu_w} \right)_{T, P, N_s} = \left( \frac{\partial \mu_s^{(\text{cav})}}{\partial \mu_w} \right)_{T, P, N_s^{(\text{cav})}} \quad (11)$$

Since the number of cavities equals the number of sites,  $N_s^{(\text{cav})} = N_s$ , integration of eq 11 leads to the following result:

$$\mu_s = \mu_s^{(\text{cav})} + C(T, P, N_s) \quad (12)$$

where  $C$  is a quantity depending on  $T$ ,  $P$ , and  $N_s$ .

In the case when intersolute interaction is negligible,  $\mu_s - \mu_s^{(\text{cav})}$  depends only on solute–solvent interaction. It follows in this case that the  $N_s$  dependence on  $C$  is negligible. It then holds that

$$\Delta \mu_s = \Delta \mu_s^{(\text{cav})} = \Delta G^*_{\text{free}} \quad (13)$$

in the absence of hydrogen bonds. In the following, we use the

(41) Schellman, J. A. *Biopolymers* **1978**, *17*, 1305.

(42) Stigler, D. J. *Phys. Chem.* **1960**, *64*, 842.

(43) Timasheff, S. N. *Biochemistry* **1992**, *31*, 9857. Timasheff, S. N. *Annu. Rev. Biophys. Biomol. Struct.* **1993**, *22*, 67.

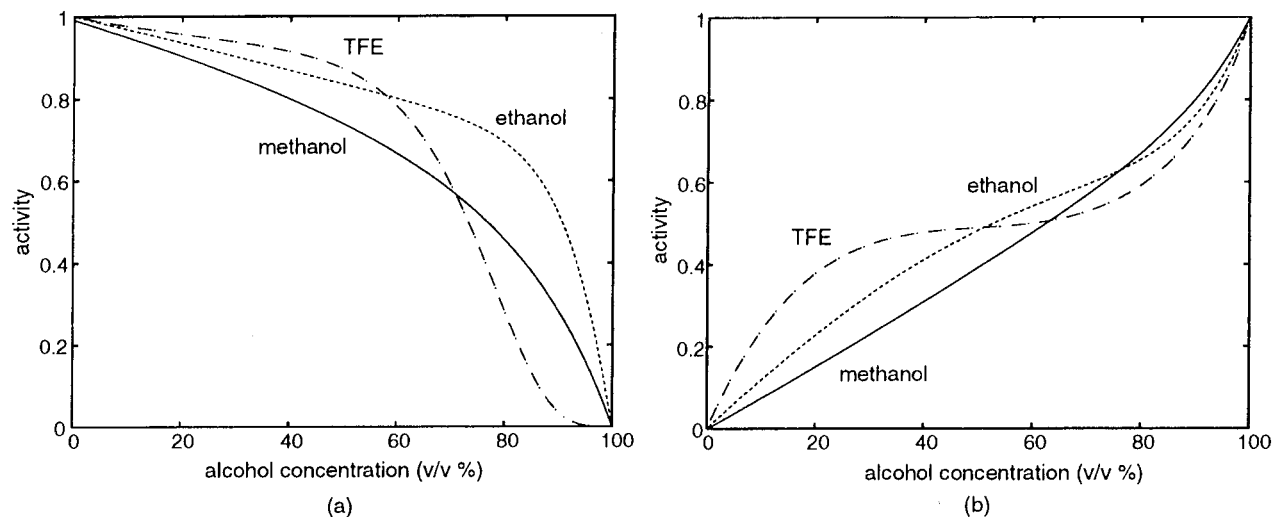


**Figure 1.** Activities of (a) water and (b) alcohols in aqueous methanol, ethanol, and TFE solutions of various solvent compositions. The data are taken from refs 32 and 33.

hard-sphere theory, namely, the SPT applicable to arbitrary molecular shape<sup>44</sup> to model free site transfer.

We must mention another assumption taken in our formalism: the intermolecular attraction between the solvent molecules are implicitly taken into account through the experimental density data of solvents; the intermolecular interaction has merely been considered as a factor that determines the density. This assumption has been supported for water in which the cavity formation can be described by SPT with experimental solvent densities, although water has a complex solvent structure due to hydrogen bonding between water molecules. We assume that SPT with experimental solvent densities also serves as a good descriptor for alcohol water mixtures. This assumption, however, should be checked by comparing simulated and calculated cavity formation free energies.

### 3. Transfer Free Energy of a Peptide Group

In this section, we reproduce the solvent composition dependence of the peptide transfer free energy from basic physicochemical data of the solvent mixture for methanol<sup>26</sup> and ethanol,<sup>25</sup> for which the experimental solubility data are available. It is shown that the excluded-volume effects play the dominant role in the low alcohol concentration range. We then calculate the transfer free energy of a peptide unit from pure water to a TFE–water mixture and incorporate the effect of conditional solvation on transfer in the presence of side chains in order to account for the observed TFE concentration dependence of helix induction. This is done in the framework of simple stoichiometric binding and successfully explains the strong helix induction by TFE.

**3.1. Calculating Transfer Free Energy of a Peptide Group from Solubility Data.** The transfer free energy of a peptide backbone from water to aqueous alcohols has been calculated from experimental solubility data of amino acids and peptides in pure water and aqueous alcohol mixture of various concentrations.<sup>2,25,26,29,45</sup> However, these calculations are based on the mole fraction concentration scale which has flaws and inconsistencies in its basis, as has been pointed out by Ben-Naim.<sup>40</sup> Instead of repeating his discussion, we only point out the

following disadvantage of the mole fraction scale: activity coefficients, which are required to incorporate nonideality in the solvation free energy have often been ignored because of experimental difficulty.<sup>29</sup> A molarity-based concentration scheme is free from these difficulties and has a clear physical meaning, i.e., the transfer free energy of a solute from a fixed position in a phase to a fixed position in another phase.

It is thus necessary to recalculate the transfer free energy of a peptide backbone in the molarity concentration scale.

The measured solubility data are tabulated in Tables 1 and 2 for methanol and ethanol solutions of various concentrations. These raw data are transformed to the transfer free energy of a molecule X (= Gly, Gly–Gly, Gly–Gly–Gly) from pure water *w* to a aqueous alcohol mixture of a concentration  $\kappa$  by the following procedure:

$$\Delta G_X(w \rightarrow \kappa) = -RT \ln(\rho_{X,\kappa}/\rho_{X,w}) \quad (14)$$

where  $\rho_{X,w}$  and  $\rho_{X,\kappa}$  respectively express the solubility of X in the solutions of *w* and  $\kappa$  in the molarity concentration scale. The measured solubilities, unfortunately, are mutually different. It is reported that different samples of amino acid may give different solubilities, due possibly to the existence of polymorphic crystalline forms<sup>27,47</sup> and this gives different solubility values in Tables 1 and 2.

From the transfer free energies of Gly, Gly–Gly, and Gly–Gly–Gly, the transfer free energy of the peptide backbone  $\Delta G_{\text{peptide}}$  is calculated by the procedure of Tanford, as

$$\Delta G_{\text{peptide}} = \Delta G_{\text{Gly-Gly}} - \Delta G_{\text{Gly}}$$

or

$$= \Delta G_{\text{Gly-Gly-Gly}} - \Delta G_{\text{Gly-Gly}}$$

or

$$= (1/2)(\Delta G_{\text{Gly-Gly-Gly}} - \Delta G_{\text{Gly}}) \quad (15)$$

Note that there are three ways of calculating  $\Delta G_{\text{peptide}}$  which may introduce scattering of the data points calculated from experimental solubility data.

(44) Boublik, T. *Mol. Phys.* **1974**, *27*, 1415.

(45) (a) Cohn, E. J.; McMeekin, T. L.; Edsall, J. T.; Weare, J. H. *J. Am. Chem. Soc.* **1934**, *56*, 2270. (b) McMeekin, T. L.; Cohn, E. J.; Weare, J. H. *J. Am. Chem. Soc.* **1935**, *57*, 626. (c) McMeekin, T. L.; Cohn, E. J.; Weare, J. H. *J. Am. Chem. Soc.* **1936**, *58*, 2173.

(46) (a) Ben-Naim, A.; Marcus, Y. *J. Chem. Phys.* **1984**, *81*, 2016. (b) Ben-Naim, A. *Solvation Thermodynamics*; Plenum: New York, 1988.

(47) Iitaka, Y. *Acta Crystallogr.* **1961**, *14*, 1.

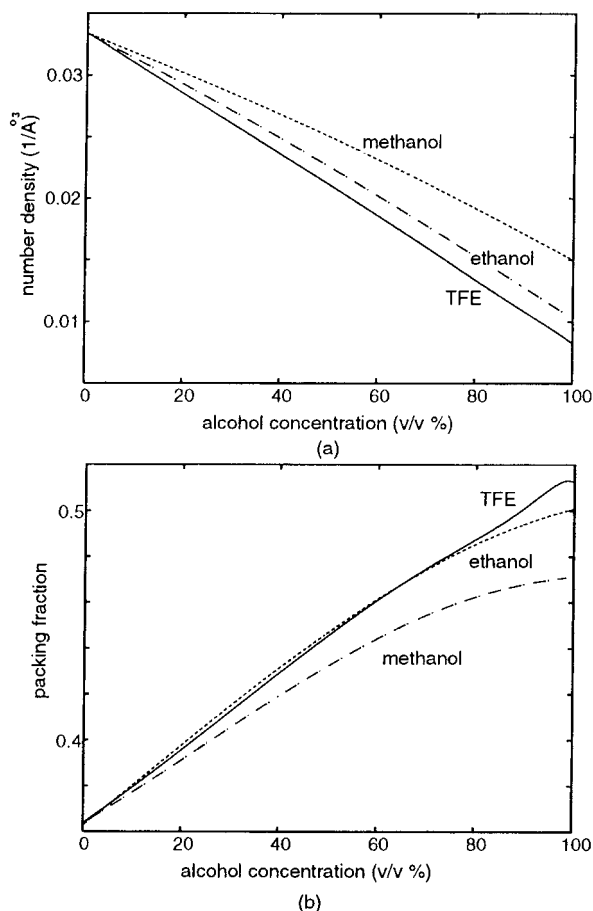


**Figure 2.** (a) Densities and (b) packing fractions of aqueous methanol, ethanol, and TFE solutions plotted against alcohol concentration. The density data are taken from refs 30 and 31.

**Table 1.** Solubilities of Glycine, Diglycine, and Triglycine in Methanol–Water Mixtures of Various Methanol Concentrations<sup>a</sup>

	methanol, % (v/v)					
	0	20	40	60	80	100
Gly	25.00	11.68	4.59	1.54	0.36	0.04
Gly–Gly	22.67	7.97	2.38	0.62	0.08	0.02

<sup>a</sup> Taken from ref 26. Solubility data from Gekko,<sup>26</sup> given in grams per 100 g of solvent.

In the evaluation of  $\Delta G_{\text{peptide}}$ , we pose the following criteria: the procedure of eq 15 should be performed within the data reported from the same group. This criterion is expected to avoid further errors introduced in the experimentally derived transfer free energy from the different values of solubilities due to the different crystalline forms used.

The results are tabulated in Tables 3 and 4. The calculated value are not significantly different from previously reported mole fraction-based free energies.<sup>25,26</sup>

The experimental transfer free energy thusly obtained is scattered as seen in Tables 3 and 4. We emphasize here the following points on the accuracy of the obtained transfer free energies: (1) errors due to the nonunique definition scatters  $\Delta G_{\text{peptide}}$ . (2)  $\Delta G_{\text{peptide}}$  becomes increasingly inaccurate at higher concentrations of the alcohols, since the solubilities of glycine decrease. Thus the reliability of  $\Delta G_{\text{peptide}}$  lies only in the lower alcohol concentrations.

**3.2 Calculating Peptide Transfer Free Energy from the Theory.** Here we will calculate the solvent composition dependence of the peptide transfer free energies for ethanol and methanol by the theory developed in section 2.

For the calculation of the free site transfer term, the volume, surface area, and mean radius of curvature of the molecular hard core of solutes and solvents should be calculated. The water molecules are assumed to be a sphere having the hard core diameter of 2.75 Å. The hard core volumes of other molecules have been calculated as follows: first, the van der Waals volume is calculated according to the additivity parameters given by Bondi<sup>51</sup> (methanol 36.0 Å<sup>3</sup>; ethanol 53.1 Å<sup>3</sup>; TFE 65.9 Å<sup>3</sup>; peptide unit 49.98 Å<sup>3</sup>). These van der Waals volumes are transformed to the hard core volumes by the regression equation given by Ben-Amotz and Willis<sup>50</sup> (the regression equation for short chain<sup>50</sup> has been used for methanol and ethanol, and the regression equation for over four heavy atoms<sup>50</sup> has been used for TFE and the peptide unit). The resulting hard core volumes are tabulated in Table 5.

The densities of the alcohol–water mixture have been taken from experimental data from various sources; ethanol–water,<sup>30</sup> methanol–water,<sup>32</sup> and TFE–water.<sup>31</sup> The number densities of each mixture as well as packing fractions calculated by using the hard core volumes of alcohol and water molecules are respectively given in parts a and b of Figure 2.

Since the alcohol molecules are nonspherical, it is required to calculate the surface areas and mean radius of curvatures of the molecules. First, we produce a molecular coordinate of the alcohols by using Mopac 6.0. We then attribute the hard core diameter of each atomic group so that the calculated volume will be equal to that of the hard core volumes obtained above. The hard core diameters for each group were as follows: methyl and methylene, 3.70 Å, which were taken to be the values given by Vega et al.,<sup>52</sup> and the rest of the groups have been obtained by fitting the molecular hard core volume, obtaining hydroxyl 2.75 Å, and trifluoroethyl 4.35 Å. The hard core surface area  $S_a$  thus obtained is tabulated in Table 5. The mean radius of curvature  $R_a$  is calculated from the analytical formula of Amos and Jackson:<sup>53</sup> the heteronuclear diatomics model was used for methanol and the heteronuclear triatomics model for ethanol and TFE. The hard core diameter of ethylene was set to be 3.70 Å (which is the same as ref 52) and trifluoromethyl group was set to 3.945 Å (which reproduces the molecular volume). The peptide unit has been assumed to be a spherical shape due to its complex shape.

All these parameters have been used in the following SPT equation of Boublik<sup>44</sup> for the calculation of the free site transfer:

$$\Delta G_{\text{free}} = -RT \ln(1 - \eta) + RT \left( \frac{R_a}{V_s/S_s} \right) \frac{\eta}{1 - \eta} + RT \left( \frac{S_a}{V_s/R_s} \right) \frac{\eta}{1 - \eta} + RT \left( \frac{R_a^2}{V_s^2/S_s^2} \right) \frac{\eta^2}{2(1 - \eta)^2} \quad (16)$$

where  $R_a$ ,  $S_a$ , and  $V_a$  and  $R_s$ ,  $S_s$ , and  $V_s$  are the mean radius of curvature, surface area, and volume of the solute and solvent molecules, respectively.

The strengths of hydrogen bonds, namely, the equilibrium constant of the following reactions,

(48) Abraham, M. H.; Berthelot, M.; Laurence, C.; Taylor, P. J. *J. Chem. Soc. Perkin Trans. 2* **1998**, 1998, 187.

(49) (a) Abraham, M. H. *Chem. Soc. Rev.* **1993**, 22, 73. (b) Abraham, M. H.; Chadha, H. S.; Whiting, G. S.; Mitchell, R. C. *J. Pharm. Sci.* **1994**, 83, 1085.

(50) Ben-Amotz, D.; Wills, K. G. *J. Phys. Chem.* **1993**, 97, 7736.

(51) Bondi, A. *J. Phys. Chem.* **1964**, 68, 441.

(52) Vega, C.; Lago, S.; Garzon, B. *J. Chem. Phys.* **1993**, 100, 2182.

(53) Amos, M. D.; Jackson, G. *J. Chem. Phys.* **1992**, 96, 4604.

**Table 2.** Solubilities of Glycine, Diglycine, and Triglycine in Ethanol–Water Mixtures of Various Ethanol Concentrations<sup>a</sup>

	ethanol, % (v/v)							
	0	20	40	50	60	80	90	100
Gly <sup>a</sup>	25.18	10.78		2.41				
Gly <sup>b</sup>	25.16	11.30	4.25	2.57	1.40	0.243	0.050	
Gly–Gly <sup>a</sup>	20.50	6.96		1.02				
Gly–Gly <sup>d</sup>	22.75	7.53	2.15		0.529	0.578		
Gly–Gly–Gly <sup>a</sup>	7.11	2.00		0.25				
Gly–Gly–Gly <sup>b</sup>	6.45	2.14	0.68		0.165			
Gly–Gly–Gly <sup>c</sup>	6.06						0.01345	8.737 × 10 <sup>-4</sup>
								2.554 × 10 <sup>-5</sup>

<sup>a</sup> Solubility data from (a) Conio et al.,<sup>28</sup> (b) Nozaki and Tanford,<sup>25</sup> (c) McMeekin et al.,<sup>45</sup> and (d) McMeekin et al.,<sup>45</sup> given in grams per 100 g of solvent.

**Table 3.** Transfer Free Energies of a Peptide Unit from Water to Methanol–Water Mixtures Recalculated in the Molarity-Based Concentration Scale<sup>a</sup>

	methanol, % (v/v)				
	20	40	60	80	100
GG–G	168.1	331.2	500.0	833.2	352.7

Data in calories per mole. Experimental solubility data from Gekko.<sup>26</sup>

**Table 4.** Transfer Free Energies of a Peptide Unit from Water to Ethanol–Water Mixtures Recalculated in the Molarity-Based Concentration Scale<sup>a</sup>

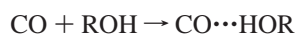
	ethanol, % (v/v)							
	20	40	50	60	80	90	100	
GGG <sup>a</sup> –GG <sup>a</sup>	111.45		205.7					
GG <sup>a</sup> –G <sup>a</sup>	137.61		387.6					
(GGG <sup>b</sup> –G <sup>b</sup> )/2	124.4		296.7					
GGG <sup>c</sup> –GG <sup>d</sup>					80.07	520.0	805.8	
(GGG <sup>b</sup> –G <sup>b</sup> )/2	89.71	139.7		230.2				

<sup>a</sup> Data in calories per mole. Experimental solubility data from (a) Conio et al.,<sup>28</sup> (b) Nozaki and Tanford,<sup>25</sup> (c) McMeekin et al.,<sup>45</sup> and (d) McMeekin et al.<sup>45</sup>

**Table 5.** Hydrogen-Bonding Strengths and Hard Sphere Parameters Used in Theoretical Calculation of Transfer Free Energies<sup>a</sup>

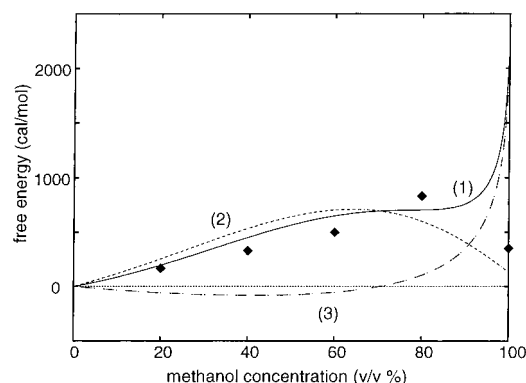
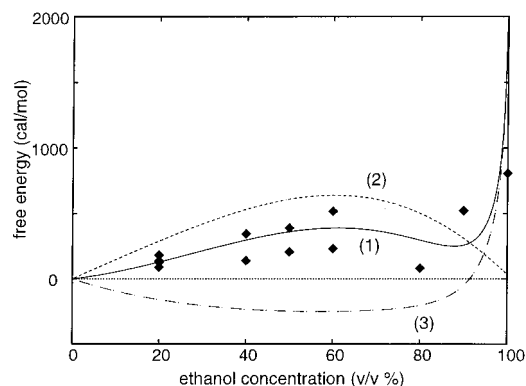
molecule	$K_{CO}^b$	$K_{NH}^b$	$V, \text{\AA}^3$	$S, \text{\AA}^2$	$R, \text{\AA}$
water	8652	7.067	10.89	23.75	2.75
methanol	101.4	15.08	31.0	48.1	4.02
ethanol	51.98	16.06	46.9	68.1	4.79
TFE	504.8	3.759	59.6	77.5	6.68
peptide			45.5	61.7	4.43

<sup>a</sup>  $K_{CO}$  and  $K_{NH}$  express the solvent molecule's binding constants to CO and NH groups, respectively. <sup>b</sup> From acidity and basicity parameters of refs 48 and 49. <sup>c</sup> Calculated by the method of ref 50. <sup>d</sup> Assuming  $R_{CH_3} = R_{CH_2} = 3.7$ ,  $R_{OH} = 2.75$ , which approximately reproduces  $V$ . <sup>e</sup> By ref 53. Equilibrium constants are dimensionless.



where R (H, methyl, ethyl, trifluoroethyl) is obtained from the acidity and basicity parameters of Abraham and co-workers.<sup>48,49</sup> These are used as parameters of the solvent-exchange term (the second term of eq 5). We have N-methylacetamide as the model compound of the hydrogen-bonding donors and acceptors of the peptide backbone. The parameters thus obtained are compiled in Table 5.

The calculated transfer free energies from water to aqueous alcohols are in good agreement with the experimental ones for methanol (Figure 3) and ethanol (Figure 4) for the lower concentration range of alcohols, but the theory appears to fail at close to 100% alcohols. As has been mentioned in section 3.2, the extremely low solubility of glycines at these concentra-

**Figure 3.** Methanol concentration dependence of peptide transfer free energy from water to methanol–water mixtures. The dots are the experimental values given in Table 3, and curve 1 is calculated from our theory. The theoretical curve (1) is made up of free site transfer (2) and hydrogen-bonding exchange terms (3).**Figure 4.** Ethanol concentration dependence of peptide transfer free energy from water to ethanol–water mixtures. The dots are the experimental values given in Table 4, and curve 1 is calculated from our theory. The theoretical curve (1) is made up of free site transfer (2) and hydrogen-bonding exchange terms (3).

tion ranges prevents one from accurately determining the experimental transfer free energy (actually, the experiments report less significant figures for the solubilities in such a range). Moreover, the theory ignores the effect of size difference between water and alcohol molecules upon the solvent-exchange reaction as well as cooperability between the reactions taking place in neighboring hydrogen-bonding sites in the peptide unit, and the theory is based on the assumption that the intermolecular interaction between solvents mainly contributes to the solvent density. Comparison between theory and experiments over the whole concentration range requires further accuracy in experiments as well as further development of the theory. However, since many denaturation experiments concentrate on the denaturation free energy at low alcohol concentration, through the use of  $m$ -values (refs 12 and 20 and references therein), the

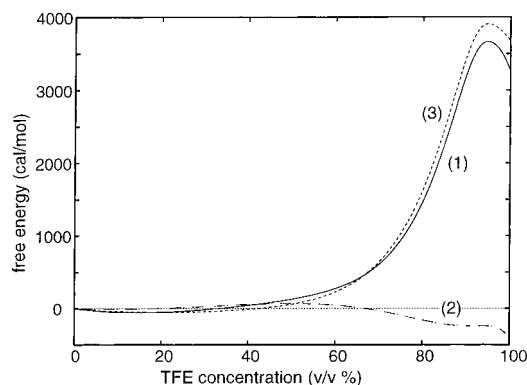


**Figure 5.** TFE concentration dependence of peptide transfer free energy from water to TFE–water mixtures calculated from theory (1), which is made up of free site transfer (2) and hydrogen-bonding exchange terms (3).

present theory covers the concentration range of major experimental interests.

The theoretical curves in Figures 3 and 4 are composed of the terms of free site transfer and hydrogen-bonding exchange. It is noteworthy that, in both cases, the dominant contribution to the transfer free energy is the free site transfer, calculated by the hard sphere theory, where interplay of molecular size effects and the packing density of the solution give the bell-shape concentration dependence as seen in Figures 3 and 4. The increase of mean solvent size upon addition of alcohols lowers the cavity formation free energy.<sup>35</sup> The increase of the packing density of the solvent upon the addition of alcohols increases the chemical potential of the solute. The excluded-volume effect thus plays a dominant role in this concentration range. The transfer free energies of peptide units in ethanol are lower than those of methanol in the corresponding alcohol concentration, despite higher packing fraction as shown in Figure 1b. This is because of the larger hydrogen-bonding exchange free energy due to the larger nonideality of ethanol in comparison to methanol, as well as smaller free site transfer free energy due to the larger molecular size of ethanol.

At the lower concentration range of TFE, the calculated transfer free energy is much lower than those for ethanol, although TFE has packing fractions comparable to that of ethanol (Figure 2b). This is due to the large size of TFE in comparison to ethanol, as was described in the Introduction. The transfer free energy rises steeply at a concentration lower than that of ethanol and methanol because the water activity dies out to zero at concentrations lower than ethanol and methanol (in this case, water molecules are strongly bound to TFE because of the inability of TFE to make intermolecular complexes by themselves<sup>23</sup>) due to the weak basicity of TFE.

It is a well-known fact that, in denaturation experiments, the denaturation free energy in TFE–water saturates at a relatively low concentration of TFE of about 40% (v/v). Figure 5, on the other hand, shows increasing transfer free energy with respect to alcohol concentration. As we discussed in the Introduction, the helix stabilization is explained by  $\Delta g_{\text{peptide}}$  in Tanford's scheme. The TFE concentration dependence shown in Figure 5 shows that Tanford's scheme does not explain the observed saturation of helicity. We must thus go beyond Tanford's scheme of group additivity by incorporating conditional solvation (i.e., solvation free energy of the peptide unit in the presence of neighboring groups).

### 3.3. Mechanism of Helix Stabilization by Trifluoroethanol.

Here we ask the question, what is the mechanism that makes the free energy of denaturation saturate at a relatively low

concentration of TFE? This question can be answered by considering conditional solvation, i.e., solvation of a peptide unit in the presence of neighboring side chains. Consideration of this effect is especially important for TFE with its large molecular size. This can be done by examining the following model. A TFE molecule bound to hydrophobic side chains of polypeptides prevents the peptide group from making hydrogen bonds with solvent molecules, which has been discussed by Rajan and Balaran<sup>23</sup> as the main factor for coil-state destabilization.<sup>17</sup> However, the quantitative explanation of the alcohol denaturation based on this picture has not been given. To describe the concentration dependence of the peptide unit solvation as the fundamental factor in the makeup of the helix induction curve, we propose the following simple stoichiometric reaction for the quantitative mode:



where we have assumed that TFE replaces three water molecules bound to the side chain  $s$  because the cross-section ratio between the two molecules is approximately 3. The equilibrium constant  $K$ , expressed as  $K = [w]^3[s \cdots \text{TFE}]/[\text{TFE}][s \cdots w_3]$ , can be estimated as follows: the hydrophobic association of two trifluoroethyl groups, whose van der Waals radii are about 4.1 Å in the mean spherical approximation,<sup>51</sup> leads to the values of a free energy 2.0 kcal/mol<sup>54</sup> and equilibrium constant of  $K = 29$ . This value is used in the subsequent applications.

Let us then model the “drying out”, i.e., shielding of the hydrogen bonds of peptide CO and NH with solvents by the TFE molecules bound to the side chain. By generalizing the formalism of section 2.1, the number density of free sites,  $[p]'_m$ , and sites bound by water  $[p \cdots w]'_m$  and alcohol  $[p \cdots a]'_m$  are expressed as,

$$\begin{aligned} [p]'_m &= [p]_m \{ 1 + (K[a]/([w]^3 + K[a])) \} \\ [p \cdots w]'_m &= [p \cdots w]_m ([w]^3 / ([w]^3 + K[a])) \\ [p \cdots \text{TFE}]'_m &= [p \cdots \text{TFE}]_m ([w]^3 / ([w]^3 + K[a])) \quad (19) \end{aligned}$$

where we have assumed that the binding of TFE to side chains completely blocks the peptide–solvent hydrogen bonds.

Since the total number of sites  $[[P]]'_m$  is written as the sum  $[[P]]'_m = [p]'_m + [p \cdots \text{TFE}]'_m + [p \cdots w]'_m$ , the transfer free energy is now expressed as,

$$\begin{aligned} \Delta G'^* &= -RT \ln \frac{[p]_m}{[p]_0} - RT \ln \left\{ 1 + \frac{K[a]}{[w]^3 + K[a]} + \right. \\ &\quad \left. \frac{[w]^3}{[w]^3 + K[a]} (K_w[w] + K_a[a]) \right\} + RT \ln(1 + K_w) \quad (20) \end{aligned}$$

The resulting peptide transfer free energy is plotted in Figure 6. A plateau at the lower TFE concentration appeared. This first plateau should be the origin of the experimentally reported saturation of helicity<sup>20</sup> at about 40% (v/v) TFE. However, it is also observed in Figure 4 that  $\Delta G'^*$  has a rise at around 70% (v/v), around which water activity dies out to zero.<sup>33</sup> This rise is probably unrealistic for the following reason: although side chain–TFE attraction is dominated by hydrophobic interactions in the water-rich region, the concentration in the TFE-rich region is due to van der Waals interaction that is expected to be much weaker than hydrophobic interaction. Therefore, the equilibrium

(54) Israelachvili, J. N. In *Intermolecular and Surface Forces*; Academic Press: London, 1992. Israelachvili, J. N.; Pashley, R. N. *Nature* **1982**, *300*, 341.

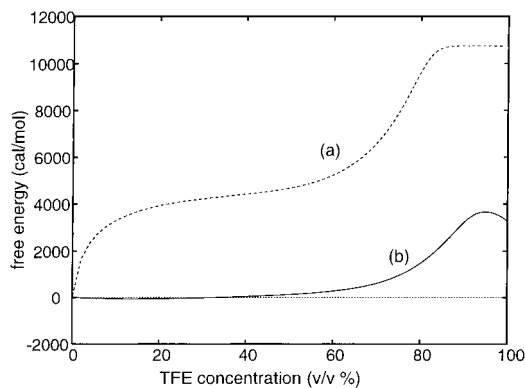


**Figure 6.** TFE concentration dependence of peptide transfer free energy from water to TFE–water mixtures calculated by assuming the effect of conditional solvation in the presence of side chains (a). Curve b is the transfer free energy of Figure 3, which assumed group additivity.

constant  $K$  determined from hydrophobic interaction is probably overestimated in the TFE-rich region. Thus we think the rise does not actually occur, and the transfer free energy converges to around 4000 cal/mol as can be expected from the TFE-rich region of Figure 3. A detailed discussion of the hydrophobic interaction in the alcohol–water mixture will clarify the above discussion. This would also clarify the TFE concentration dependence of side chain–side chain hydrophobic attraction in the helix state. It is noteworthy, however, that the calculation of Figure 6a was based on the assumption that the peptide–solvent hydrogen bonds are completely shielded by TFE bound to side chains. The concentration dependence of actual peptide transfer falls between the curves a and b, with the plateau caused by shielding. Quantitative treatment of real polypeptides requires the consideration of the actual shielding ratio. However, the discussion in this paper qualitatively explains the physical origin of the saturation behavior of the TFE denaturation curve.

We ask one final question: why is TFE a strong helix stabilizer? The large transfer free energy of a peptide unit in the absence of conditional solvation partly explains the strong helix stabilization effect. However, a comparison of Figures 3 and 4 shows that the steep increase of  $\Delta G^*$  with respect to TFE concentration at the water-rich region results from an increasing bonding of TFE to the side chain, which comes from the steep rise in TFE activity with respect to TFE concentration.<sup>33</sup> This is, from a molecular point of view, due to low basicity of TFE<sup>23,49</sup> (see Table 3); i.e., the low basicity of TFE makes its fugacity higher than that of an ideal solution in the water-rich region. To summarize, the poor basicity of TFE, side chain–TFE hydrophobic bonding, and the large excluded-volume effect of aqueous TFE are the factors that make TFE a strong helix stabilizer.

#### 4. Conclusion

In this paper, we have developed a general theoretical scheme that enables us to calculate transfer free energies of a peptide unit from pure water to various alcohol–water solvent compositions based on the molarity-based pseudochemical potential of Ben-Naim.<sup>40</sup> Two main contributions to the transfer free energy are the free site transfer, which was shown to be modeled by hard sphere theory, and the peptide–solvent hydrogen bonds, which can be modeled by the solvent-exchange formalism of Schellman.<sup>39</sup> This theory can reproduce the transfer free energy of the peptide unit (recalculated from solubility data in the molarity-based concentration scale) for methanol and ethanol at lower alcohol concentrations. The physical picture extracted from this theoretical reproduction is that the excluded-volume effect plays a dominant role, where the interplay between molecular size effects and solvent density is the important factor.

The transfer free energy of the peptide unit from water to TFE–water was calculated by the theory developed in this paper. The transfer free energy is much larger than in ethanol and methanol; the molecular picture of this has been explained in terms of the solvent structure of the alcohol–water mixture. However, the transfer free energy in TFE–water as shown in Figure 3 does not represent the concentration dependence where, as has been reported by experiments, helicity is saturated at relatively low TFE concentrations. To explain the saturating behavior of the free energy of denaturation of peptides and proteins at a low concentration of TFE, we included the effect of conditional solvation, i.e., the effect of TFE bound to the hydrophobic side chains on the solvation of peptide units. With the stoichiometric binding model of hydrophobic bonding, and its effect on the peptide drying out (i.e., shielding peptides from hydrogen bonds to the solvent molecules), we were able to derive the saturation of peptide transfer free energy at low TFE concentration. From these examples, it is shown that our theory could describe the solvent composition dependence of the peptide unit solvation, which is the fundamental contribution to the alcohol denaturation.

**Acknowledgment.** We thank Professors K. Nagayama and Y. Goto, Mr. M. Arai, Ms. N. Hirota-Nagaoka, and Dr. M. Ikeguchi for many stimulating discussions. Professor M. Uematsu has kindly sent us the list of references for the TFE–water mixture. S.S. is grateful to Kaori Sakurai for continuous encouragement.

JA982560S